International Journal of GEOMATE, July, 2018 Vol.15, Issue 47, pp.95-102
Geotec., Const. Mat. & Env., DOI: https://doi.org/10.21660/2018.47.7171
ISSN: 2186-2982 (Print), 2186-2990 (Online), Japan

HYPERBOLIC MODEL PARAMETERS OF PHILIPPINE COAL ASH

* Erica Elice Saloma Uy [1] and Jonathan Rivera Dungca [2]

[1]Graduate Student, De La Salle University, Philippines; [2] De La Salle University, Philippines

*Corresponding Author, Received: 8 July 2017, Revised: 20 Dec. 2017, Accepted: 20 Feb. 2018

ABSTRACT: In the 2016 Annual Energy Sector accomplishment report of the Philippine's Department of Energy, power generation in the Philippines relied on the coal-fired power plant at 46%. An increase of 19.47% was observed from 2003 to 2016. The increase in demand would result in an increase in production of waste material from the power plant namely, coal ash. Furthermore, the disposal of these waste materials can be an issue because it can cause a shortage in storage facilities. To address this, there is a need to study on the possibility of reusing these waste materials. A probable use of the waste material is by using it as a construction material for road embankments. In the Philippines some of these structures are constructed on areas exposed to seawater in order to address traffic congestion. This study proposes to use coal ash as the material for road embankment. Triaxial test under consolidated drained condition was performed considering the exposure to seawater. Three conditions were implemented namely, no exposure, immediate exposure and prolonged exposure. Based on the results, 100% fly ash had the highest strength. The hyperbolic model was employed to simulate the material's stress-strain response. The hyperbolic model was chosen since it has the capability of predicting the load-displacement behavior of the waste material under monotonic loading. The Hyperbolic model prediction shows that the material can still handle higher stresses. With this, the ash mixtures tested has a potential to be used as a construction material for a road embankment.

Keywords: Coal ash, Hyperbolic model, Construction material, Road embankment

1. INTRODUCTION

According to the Annual Energy Sector accomplishment report of the Philippine's Department of Energy, power generation grossed at 42,700 Gigawatt hours (GWh) in the first semester of 2016 [1]. Coal-fired power plant generated power at 19,695 GWh. It was followed by renewable energy, natural gas and oil-based power plant at 10,158 GWh, 10,141 GWh and 2, 705 GWh, respectively. In the report, coal-fired power plant remains the major source of electricity at 46 %. In the same year, coal production for the first three quarter reached 8.4 million metric tons (MMMT). In the recent Summary of Installed Capacity, Dependable Capacity, Power Generation and Consumption report of the Department of Energy which was published on March 27, 2017, an increase of 19.47% in contribution to the power generation mix was observed from 2003 to 2016 [2]. The increase in demand would result in an increase in production of waste material from the power plant namely, coal ash. Furthermore, the disposal of these waste materials can be an issue because it can cause a shortage in storage facilities such as ash pond.

Using coal ash as a construction material has been a trend in the construction industry due to its abundance. The most frequently used coal combustion by-products (CCB) or coal ash by-products are fly ash and coal ash [3]. Fly ash has been used as a material for cement, concrete and grout production, road embankment, reclamation and structural fill [3], [4], [5], [7], [20], [21]. It was proven that the partial replacement of fly ash to cement can reduce the demand for water and it improves the concrete's workability. Furthermore, due to its abundance it is an economical material especially for road embankments and reclamation projects [4], [5]. Bottom ash on the other hand was found to have similar performance when compared with typical highway materials. More so, it also meets the conventional materials' specifications and can be used as subgrade and subbase [6]. To further utilize these by-products or waste materials' capability, mixture proportions were tested as a possible construction material for highway embankments. A study investigated 3 mixture ratios such as 50% fly ash and 50% bottom ash, 75% fly ash and 25% bottom ash and 100% fly ash. Based on their results, the mixture ratio of 50% fly ash and 50% bottom ash had the highest peak angle of internal friction are suitable for highway embankments. In addition, the results of the study were also in good agreement with the strength and compressibility specifications of a typical fill material [7]. Another study conducted a field performance investigation on a 60% fly ash and 40% bottom ash mixture for a construction of an embankment. The construction was monitored to determine the behavior and performance of the material used. Results showed that the ash mixture adopted is an acceptable material for embankment construction [3]. Although there are several types of research on the uses of coal ash, such as road embankment, there is still limited knowledge on its performance when it is exposed to sea water. This scenario must be considered especially in the Philippines were road embankments are now being constructed on bodies of water, such as the sea, because of traffic congestion. Some projects are the Manila-Cavite Expressway (CAVITEX) and Cebu-Cordova Link Expressway (CCLEX) [8], [9]. With this, there is a need to study on the possibility of reusing these waste materials as a construction material for road embankments exposed to seawater. It is the objective of this study to determine the performance of coal ash as a construction material considering ash mixtures such as 100% fly ash (S1), 100% bottom ash (S2) and 50% fly ash 50% bottom ash (S3). Consolidated drained triaxial test was performed and the waste material will be exposed to seawater. The samples were exposed to seawater under three conditions namely, no exposure (C1), immediate exposure (C2) and prolonged exposure (C3). To simulate the material's stress-strain response hyperbolic model was employed. The hyperbolic model was chosen since it has the capability of predicting the load-displacement behavior of the waste material under monotonic loading.

2. INDEX PROPERTIES OF COAL ASH

The coal ash used in the study is from a power plant in the central Philippines. The index properties of S1, S2 and S3 are determined following the American Society for Testing Materials and the results are tabulated in Table 1. It can be seen that all samples are non-plastic. The value of the specific gravity of the ash mixtures is higher than the recommended values ranging from 1.899 to 1.903 [10]. A possible explanation for the difference is both materials came from a different coal-fired power plant. For the results of S3, it is noticeable that the values are in between S1 and S2.

3. EXPERIMENTAL PROGRAM

3.1 Sea water Preparation

The artificial sea water used in the experiment is prepared following ASTM D 1141 – 98 or "Standard Practice for the Preparation of Substitute Ocean Water". The chemical compositions for the artificial se water are tabulated in Table 2.

Table 1 Index properties of ash mixtures

Index Property	S1	S2	S3
Specific gravity(Gs)	2.08	2.25	2.11
Liquid limit(LL)	-	-	-
Plastic limt (PL)	-	-	-
Maximum void ratio (e_{max})	1.75	0.94	1.14
Minimum void ratio (e_{min})	1.45	0.85	0.94
Maximum dry unit weight(γ_{dmax}) (kN/m^3)	9.9	13.94	11.7
Optimum water content (ω_{opt}) (%)	36.6	15.85	27.1
USCS	ML	SM	

Table 2 Chemical composition of sea water

Compound	Concentration,g/L
NaCl	24.53
MgCl	5.2
NaSO	4.09
CaCl	1.16
KCl	0.695
NaHCO	0.201
KBr	0.101
HBO	0.027
SrCl	0.025
NaF	0.003
Ba(NO	9.94E-05
Mn(NO	3.40E-05
Cu(NO	3.08E-05
Zn(NO	9.60E-06
Pb(NO	6.60E-06
AgNO	4.90E-07

3.2 Sample Preparation

The ash mixtures were prepared by moist tamping. Instead of using relative density as the controlled variable for the initial target condition, relative compaction was preferred to properly simulate site conditions. A value of 95% relative compaction was the target initial value in order to satisfy the desired in situ conditions [7], [11]. The extent of sea water exposure for the experiment has three conditions. The first condition (C1) has no sea water exposure. Only distilled water was used and the samples were soaked for 16 hours. The second condition (C2) sample preparation is similar with C1. Sea water exposure was performed during consolidation stage of the Consolidated Drained Test. The third condition (C3) is when distilled water was completely replaced with artificial sea water both in the sample preparation step and the consolidation stage of the Consolidated Drained Test.

3.3 Consolidated Drained Test

Consolidated Drained Test or slow test was performed in this study following British Standard (BS) 1377-8: 1990. Saturation, consolidation and shear are the stages in this test. For the saturation stage, the sample must reach a fully saturated condition before it is to be consolidated. To ensure a fully saturated condition the B-value or the ratio of the change in pore water pressure and change in confining pressure must reach a value greater than 0.95. For the consolidation stage, the confining pressures (σ_3) used are 50 kPa, 100 kPa, and 200 kPa. For the shearing stage, a rate of loading of 0.05 mm/min was implemented. This was used for the proper dissipation of pore water pressure. Due to the slow rate, this stage normally performed for a maximum of 7 hours and a minimum of 4 hours.
A total of 51samples were tested for this study as shown in Table 3. It can be seen that sample S3 was not tested for the C3 condition. During sample preparation when the artificial sea water was mixed with S1 some samples hardened into a rock-like state. This made it difficult for S1 to be mixed with S2.

Table 3 Design of experiment

Ash Mixtures	Sea Water Exposure								
	C1			C2			C3		
	σ_3 (kPa)								
	1	2	3	1	2	3	1	2	3
S1	3	3	3	2	2	2	1	1	1
S2	3	3	3	2	2	2	1	1	1
S3	3	3	3	2	2	2	-	-	-

4. HYPERBOLIC MODEL

Hyperbolic model or Duncan and Chang model is an incremental stress-dependent model that is based on the stress and strain's hyperbolic relationship [13]. The soil model can simulate the non-linear response of soil. It is also a variable-parameter model and it is defined in terms of the initial tangent modulus (E_i), actual deviator stress at failure $(\sigma_1 - \sigma_3)_f$ and failure ratio (R_f) [12], [13]. The parameters in this model can be determined by performing a triaxial test [12], [13], [14]. From the variables obtained in the model, prediction of the load-displacement behavior of the soil can be performed. The hyperbolic representation of the soil model has the capability to yield acceptable results especially in cases under monotonic loading [14]. A typical result of this model is shown in Fig. 1. The hyperbola in the figure can be mathematically written as [12]:

$$\sigma_1 - \sigma_3 = \frac{\varepsilon}{\frac{1}{E_i} + \frac{\varepsilon}{(\sigma_1 - \sigma_3)_u}} \tag{1}$$

Where:
ε = axial strain
$(\sigma_1 - \sigma_3)_u$ = ultimate deviator stress

The hyperbola produced by the model in Fig. 1 is acceptable only until point A. This point is the actual deviator stress at failure. It can be used to define the failure ratio together with the ultimate deviator stress. The typical values for the failure ratio range from 0.75 to 1.0 [16]. The failure ratio is defined as:

$$R_f = \frac{(\sigma_1 - \sigma_3)_f}{(\sigma_1 - \sigma_3)_u} \tag{2}$$

The ultimate deviator stress, as seen in Fig. 1, is asymptotic in nature. Its value when compared to the compressive strength of the soil is always larger [14]. In order to establish the parameters needed in the soil model, the stress-strain plot must be transformed into a linearized hyperbolic form. The axial strain must be divided by the deviator stress and it is plotted against the axial stress. The equation of the straight line in the transformed plot is [12]:

$$\frac{\varepsilon}{\sigma_1 - \sigma_3} = \frac{1}{E_i} + \frac{\varepsilon}{(\sigma_1 - \sigma_3)_u} \tag{3}$$

Equation (3) presented is the modified format of Eq. (1). In Eq. (3), the initial tangent modulus is the reciprocal of the y-intercept while ultimate deviator stress is the reciprocal of the slope. In order to perform the prediction of the stress-strain behavior of the soil, the primary loading modulus (K) and exponent number (n) must be also established. These parameters are related to initial tangent modulus as seen in the following equation [12]:

$$E_i = K P_a (\sigma_3 / P_a)^n \tag{4}$$

Where:
Pa = atmospheric pressure (Pa = 101.325 kPa)

Based on the study of Janbu, the increase in confining pressure is proportional to the initial tangent modulus [14].

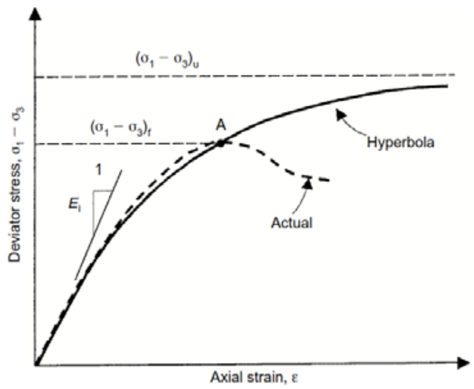

Fig.1 Hyperbolic model prediction typical result [12]

The parameters primary loading modulus and exponent number can be determined from a logarithmic plot of E_i /Pa against σ_3/Pa. The plot is linearized in order to extract the mentioned parameters. The equation of the straight line can be written as follows [12]:

$$\log_{10}\left(\frac{E_i}{P_a}\right) = \log_{10}(K) + n\log_{10}\left(\frac{\sigma_3}{P_a}\right) \tag{5}$$

The slope of Eq. (5) is the exponent number while the y-intercept is the primary loading modulus when σ_3/Pa is equal to 1.0. Once the hyperbolic parameters are established a prediction of the load-displacement behavior of the soil can be performed by using the following equation [12], [13]:

$$\sigma_1 - \sigma_3 = \frac{\varepsilon}{\dfrac{1}{KP_a(\sigma_3/P_a)^n} + \dfrac{\varepsilon R_f(1-\sin\phi)}{2C\cos\phi + 2\sigma_3\sin\phi}} \tag{6}$$

Where:
C = cohesion
ϕ = angle of internal friction

The values of cohesion and angle of internal friction can be determined by plotting the Mohr's Circle. The deviator stress from the stress-strain plot must be at the peak state. If peak state is not experienced, the deviator stress at 15% of the axial strain can be used.

5. SHEAR STRENGTH OF ASH MIXTURES

The shear strength of ash mixtures was determined from the results of the Consolidated Drained Test. The results are tabulated in Table 4. The results were compared to the typical values of previous researches. The typical values for the angle of internal friction and cohesion for silt are 30° to 35° and 9 kPa, respectively. For silty sand, the typical values for the angle of internal friction and cohesion are 26° to 35° and 50 kPa, respectively [17], [18], [19]. For S1 it was compared to the typical values of silts while for S2 it was compared with silty sand. The results of S3 on the other hand were compared to silty sand. For the results of the ash mixtures in C1, it was observed that all the results are in good agreement for cohesion. For its angle of internal friction, the result of S1 is slightly higher than the typical value of 10%. The increase was due to the amount of relative compaction which contributed to the increase in strength of the ash mixture. It was also observed that S1 has a higher of the value of the angle of internal friction compared to S2. This is because the particle shape of the two was different. A flaky particle shape was observed for S2 while a rounded shape was for S1. The particle shape for S2 is weaker compared to S1. For S3, its values are in between S1 and S2. For the results of C2, it can be seen that the values of the angle of internal friction decreased for all ash mixtures but the values are still within the typical values. The values for cohesion on the other hand increased. This can be due to the effect of sea water used in the consolidation stage. For the results of C3, the angle of internal friction of S2 is comparable to the results at C1. For cohesion, it dramatically decreased and it is the smallest value when compared to all the results.

Table 4 Shear strength of ash mixtures

Seawater Exposure	Ash Mixture	ϕ	Cohesion (kPa)
C1	S1	38.53	8.65
	S2	33.77	28.56
	S3	38.94	8.13
C2	S1	31.95	33.32
	S2	27.03	49.91
	S3	31.86	19.06
C3	S1	-	-
	S2	33.91	15.43
	S3	-	-

6. HYPERBOLIC MODEL PARAMETERS

The hyperbolic model parameters for ash mixtures are tabulated in Table 5, 6, 7 and 8. In order to determine these parameters, the stress-strain plot was linearized as shown in Fig. 2. The plot shown is the typical result for the ash mixtures tested. It was observed that as the confining pressure increases the ratio between the axial strain and deviator stress decreases. This can also lead to the decrease in the value of the slope but the increase in the value of the ultimate deviator stress.

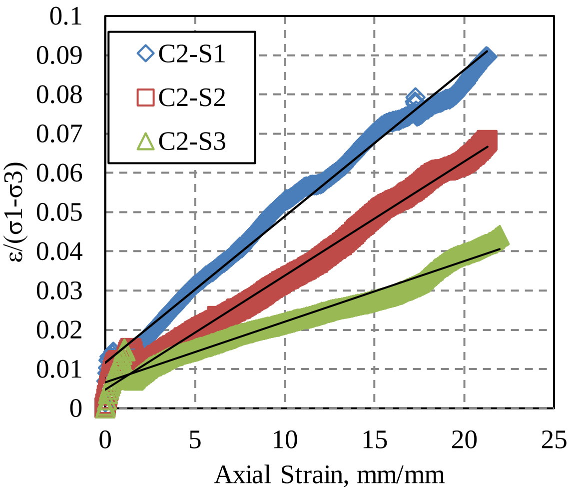

Fig.2 Typical results for linearized plot

From the tabulated results, it showed that as the confining pressure increases the ultimate deviator stress also increases. Comparing the results of the three conditions of sea water exposure, it was observed that the exposure of sea water had an effect towards the ultimate deviator stress of the ash mixtures. Based on the results in Table 7, the values of C3-S2 at 50 kPa and 100 kPa are in between the results of C1-S2 and C2-S2 under the same confining pressure. For C3-S2 at 200 kPa the results are larger than C2-S2 but smaller than C1-S2. At this confining pressure, the exposure to sea water improved the strength of the ash mixture. When the results of C1-S1 and C2-S1 were compared, it was observed that the values of ultimate deviator stress are larger for C2-S1 at 50 kPa and 200 kPa but a smaller value was observed for 100 kPa. For the results of C1-S3 and C2-S3, it can be seen that the ultimate deviator stress decreased due to sea water exposure. Comparing the results of the ash mixtures in each condition of sea water exposure, for C1 it was observed that there is no particular trend when it comes to the changes in the value of ultimate deviator stress. On the other hand for C2, it was observed that S3 had the smallest values. Knowing the values of ultimate deviator stress can serve as the upper limit or maximum strength of the ash mixtures. There was no consistent trend observed in the result of the ultimate deviator stress. This can be due to the method of sample preparation since preparing the exact replica of the relative compaction is somewhat difficult. For the result of initial tangent modulus, there is also no definite trend. This parameter is highly dependent on the behavior of the stress-strain results. When strain hardening is more pronounced prior to failure the value of initial tangent modulus is smaller. This occurred in C2-S2 at 50 kPa confining pressure. For the failure ratio, it can be observed that almost all the failure ratio is within its acceptable range which except the result from C1-S2. Its value is 0.5335. It was observed that for this ash mixture, the ultimate deviator stress is high and its deviator stress at failure is almost half of its value. This means that for its transformed plot the slope is very steep. A steep plot indicates that strain hardening was present in the stress-strain diagram. Once the hyperbolic parameters are established, prediction can now be performed using Eq. (6). The typical results are shown in Fig. 3a-c and 4a-c. Three trends were observed from the results. First, the prediction seemed less accurate as the confining pressure is increasing as seen in Fig. 3a-c. This trend was observed for all results in C1. Second, the prediction was in good agreement with some parts of the stress-strain plot such as the strain hardening portion and the behavior of the plot until it reaches the ultimate shear strength as seen in Fig. 4a-c. Third, the model cannot predict the post peak strain behavior of the ash mixtures.

Table 5 Hyperbolic parameters for C1

Ash Mixture	σ3 (kPa)	$(\sigma_1\text{-}\sigma_3)_f$ (kPa)	$(\sigma_1\text{-}\sigma_3)_{ult}$ (kPa)	E_i (kPa)	R_f
S1	50	191.93	192.31	217.39	0.9980
	100	398.15	400.00	625.00	0.9954
	200	619.39	625.00	1000.00	0.9910
S2	50	238.04	238.10	277.78	0.9998
	100	274.24	294.12	181.82	0.9324
	200	666.87	1250.00	90.09	0.5335
S3	50	207.25	208.33	769.23	0.9948
	100	470.41	476.19	102.04	0.9877
	200	688.77	909.09	136.99	0.7577

Table 6 Hyperbolic parameters for C2

Ash Mixture	σ3 (kPa)	$(\sigma_1\text{-}\sigma_3)_f$ (kPa)	$(\sigma_1\text{-}\sigma_3)_{ult}$ (kPa)	E_i (kPa)	R_f
S1	50	239.77	256.41	416.67	0.9351
	100	305.66	344.83	126.58	0.8864
	200	579.76	666.67	185.19	0.8696
S2	50	244.62	270.27	86.21	0.9051
	100	320.07	344.83	250	0.9282
	200	553.92	666.67	149.25	0.8309
S3	50	181.76	181.82	370.37	0.9997
	100	287.47	333.33	116.28	0.8624
	200	474.37	476.19	526.32	0.9962

Table 7 Hyperbolic parameters for C3

Ash Mixture	σ3 (kPa)	$(\sigma_1\text{-}\sigma_3)_f$ (kPa)	$(\sigma_1\text{-}\sigma_3)_{ult}$ (kPa)	E_i (kPa)	Rf
S2	50	187.66	188.68	185.19	0.9946
	100	248.44	270.27	129.87	0.9192
	200	586.24	714.29	153.85	0.8207

Table 8 Primary loading modulus and exponent number for ash mixtures

Seawater Exposure	Ash Mixture	K	n
C1	S1	461.42	5.57
	S2	5.99	1.34
	S3	25.99	4.50
C2	S1	10.75	1.65
	S2	5.99	1.34
	S3	37.19	1.11
C3	S1	-	-
	S2	4.66	0.22
	S3	-	-

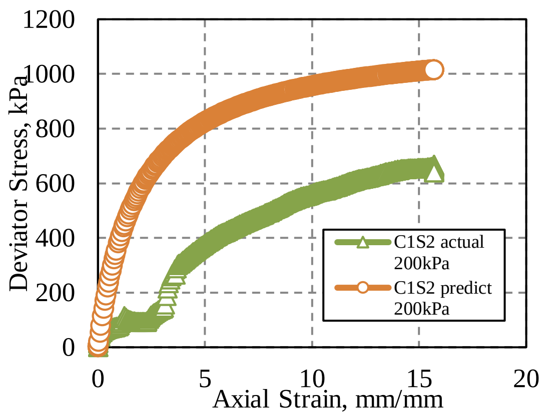

Fig.3a Hyperbolic prediction for C1-S2

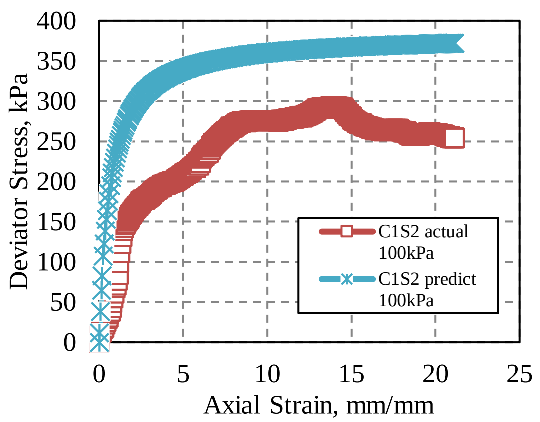

Fig.3b Hyperbolic prediction for C1-S2

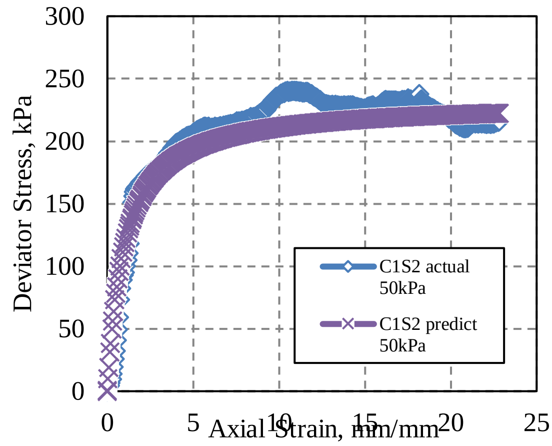

Fig.3c Hyperbolic prediction for C1-S2

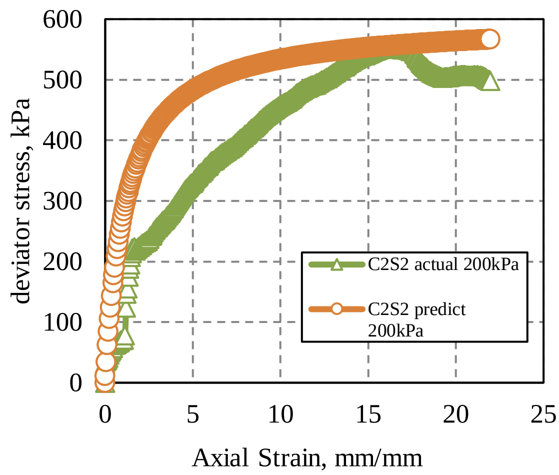

Fig.4a Hyperbolic prediction for C2-S2

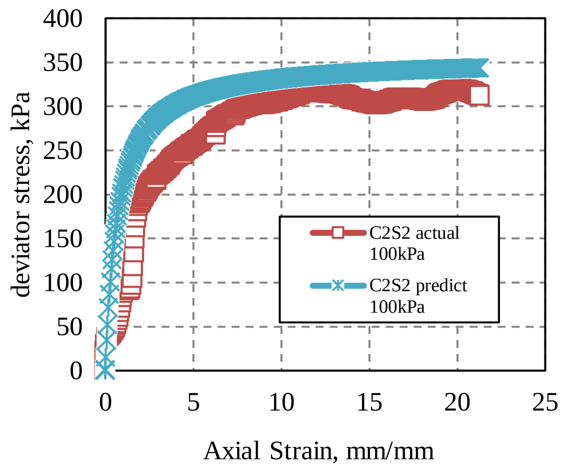

Fig.4b Hyperbolic prediction for C2-S2

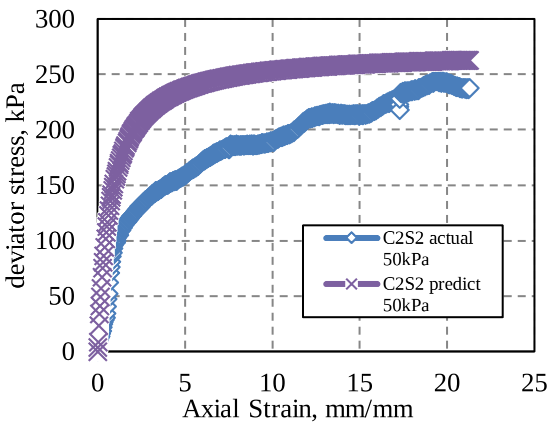

Fig.4c Hyperbolic prediction for C2-S2

7. CONCLUSION

Ash mixtures were tested under Consolidated Drained test. Three ash mixtures were considered namely, 100% fly ash (S1), 100% bottom ash (S2) and 50% fly ash 50% bottom ash (S3). These ash mixtures were exposed to sea water during the triaxial test. This was done to determine the effect of sea water towards the strength of ash mixtures. Three exposures to sea water conditions were simulated in the experiment namely, no exposure (C1), immediate exposure (C2) and prolonged exposure (C3). Based on the results, the shear strength of the ash mixtures are all within the typical values and are considered to have sufficient strength. For the exposure of sea water, it decreased the strength but the values are still within the acceptable limit. Among all the ash mixtures, S1 had the highest strength. When 50% of S1 was mixed with 50% of S2 to form S3 it showed an improvement in the strength of S3. Furthermore, it was observed that the exposure of sea water had an effect towards the values of the deviator stress at failure and ultimate deviator stress of the ash mixtures. For the C2 condition, both values for S2 and S3 mixtures are smaller compared to C1 and C3 condition. For the hyperbolic parameters, it can be seen that C1-S2 had the highest ultimate deviator stress at 200kPa. The value of the initial tangent modulus ranged from 86.21 to 1000 kPa. The hyperbolic parameters were used in predicting the stress-strain behavior of the ash mixtures. The prediction shows that the material can still handle higher stresses. The limitation of the model is that it cannot predict the post peak strain behavior. Based on the results from the Consoldiated Drained test and Hyperbolic model, they showed that the ash mixtures has a potential to be used as a construction material for a road embankment.

It is suggested that other percentages of ash mixtures be tested in order to determine the most suitable ash mixture. It can be noted that the fly ash specimen has a larger strength, increasing it might improve the strength of the ash mixture.

8. ACKNOWLEDGEMENTS

I would like to thank Dr. Jonathan R. Dungca for his encouragement, support, and technical guidance in completing this study. I would also like to thank the Civil Engineering Department of De La Salle University for their support.

9. REFERENCES

[1] Department of Energy. (2016). 2016 major accomplishments. Retrieved from http://www.doe.gov.ph/sites/default/files/pdf/transparency/annual_report_esar_2016.

[2] Department of Energy. (2017). Summary of installed capacity, dependable capacity, power generation and consumption report of the department of energy, Retrieved from https://www.doe.gov.ph/sites/default/files/pdf/energy_statistics/summary_2016_power_statistics_final_march_27_2017.pdf.

[3] Yoon, S., Ph, D., Balunaini, U., Yildirim, I. Z., Prezzi, M., & Siddiki, N. Z. (2009). Construction of an embankment with a fly and bottom ash mixture : field Pperformance study, Journal of Materials in Civil Engineering, 21, 271–278.

[4] Yao, Z. T., Ji, X. S., Sarker, P. K., Tang, J. H., Ge, L. Q., Xia, M. S. & Xi, Y. Q. (2015). A comprehensive review of the applications of coal fly ash. Elsevier, Earth-Science Reviews, 141, 105-201.

[5] Ahmaruzzaman, M. (2010). A review on the utilization of fly ash. Progress in Energy and Combustion Science, 36(3), 327-363. Elsevier Ltd. doi:10.1016/j.pecs.2009.11.003

[6] Huang, W. H. (1990). The use of bottom ash in highway embankments, subgrades and subbases. Retrieved from docs.lib.purdue.edu/cgi/viewcontent.cgi?article=1782&context=jtrp.

[7] Kim, B., Prezzi, M., & Salgado, R. (2005). Geotechnical Properties of Fly and Bottom Ash Mixtures for Use in Highway Embankments, Journal of Geotechnical and Geoenvironmental Engineering, 131(7), 914-924.

[8] CAVITEX (2016). Cavitex expressway. Retrieved from http://cavitexpressway.com/

[9] Philippine News Agency (2017). Construction of CCLEX paves way for more bridges linking Visayas islands. Retrieved from http://news.mb.com.ph/2017/03/04/construction-of-cclex-paves-way-for-more-bridges-linking-visayas-islands/

[10] Antonio, O. V. M., & Zarco, M. A. H. (2007). Engineering properties of Calaca Batangas bottom ash, 28(1), 37–56.

[11] Zabielska-Adamska, K. (2006). Shear strength parameters of compacted fly ash–HDPE geomembrane interfaces. Geotextiles and Geomembranes, 24(2), 91–102. doi:10.1016/j.geotexmem.2005.11.006.

[12] Al-shayea, N., Abduljauwad, S., Bashir, R., Al-Ghamedy, H. & Asi, I. (2001). Determination of parameters for a hyperbolic model of soils from the eastern province of Saudi Arabia. Proceedings of the Institution of Civil Engineers. (4). 1-14.

[13] Stark, T. D., Ebeling, R. M. & Vettel, J. J. (1992). Hyperbolic stress-strain parameters for silts. Journal of Geotechnical Engineering. 120(2). 420-441.

[14] Abdul-kareem, A. H. & Helal, A. (2007). Estimation of hyperbolic stress-strain parameters for gypseous soils. International Journal of Civil Engineering. (7).

[15] Tatsuoka, F. & Shibuya, S. (1991). Modelling of non-linear stress-strain relations of soils and rocks part 1, discussion of hyperbolic equation. Seisan-Kenkyu. 43(9). 23-26.

[16] Chen, W. F. & Saleeb, A. F. (1994). Constitutive equations for engineering materials. Elsevier. 1. 517.

[17] Das, B. & Sobhan, K. (2014). Principles of Geotechnical Engineering Sixth Edition, United States: Chris Carson.

[18] Geotechdata (2013). Soil friction angle. Retrieved from http://www.geotechdata.info/parameter/angle-of-friction.html.

[19] Geotechdata (2014). Soil cohesion. Retrieved from http://www.geotechdata.info/parameter/cohesion.html.

[20] Uy, E. E. S. & Dungca, J. R. (2017). Constitutive modeling of coal ash using modified cam clay model. International Journal of GEOMATE, 12(31), 88-94.

[21] Dungca, J. R. & Jao, J. A. L. (2017). Strength and permeability characteristics of road base materials blended with fly ash and bottom ash. International Journal of GEOMATE, 12(31), 9-15.